Opto-Electronics Review 28 (2020) 203-212

PAN POLISH ACADEMY OF SCIENCES

Opto-Electronics Review

journal homepage: http://journals.pan.pl/opelre

Dimming control schemes combining IEEE 802.15.7 and SC-LPPM modulation schemes with an adaptive M-QAM OFDM for indoor LOS VLC systems

Nazmi A. Mohammed [a], Kareem A. Badawi [a,b], Ashraf A. M. Khalaf [b], S. El-Rabaie [c]

[a] Photonic Research Lab, Electrical Engineering Department, College of Engineering, Dawadmi, Shaqra University, 11961 Kingdom of Saudi Arabia. OSA Member.
[b] Faculty of Engineering, Minia University, P.O. Box 61111, Minia, Egypt.
[c] Dept. of Electronics and Communication Eng., Faculty of Electronic Eng., Menoufia University, Qism Shebeen El-Kom, Shibin el Kom, Menofia, Egipt.

Article info

Article history:
Received 29 Aug. 2020
Accepted 08 Oct. 2020

Keywords:
visible light communication, sub-carrier pulse position modulation, lightning topologies, bit error rate

Abstract

The presented work proposes a new dimming control schemes for indoor visible light communication which combines variable pulse-position modulation, colour shift keying as key schemes of IEEE 802.15.7 standard, and sub carrier-pulse-position modulation as a pulse-position modulation variant with orthogonal frequency division multiplexing. These schemes are then compared with traditional merging schemes utilizing pulse-width modulation and multiple pulse-position modulation with m-ary quadrature amplitude modulation OFDM. The proposed schemes are investigated in a typical room with a different lighting layout (i.e., distinctive and uniform lighting layout), followed by an illumination investigation to evaluate the performance of the proposed schemes, especially the enhanced achieved data rates, and to determine their limitations as reliable visible light communication systems that can satisfy both communication and illumination requirements.

1. Introduction

The number of wireless mobile devices increases rapidly, which leads to a noticeable expansion in the wireless data traffic, which raises the need for visible light communication (VLC) technology. VLC technology witnessed a significant interest in development and research at a worldwide scale as a reliable supplement to radio frequency (RF) technology [1,2].

VLC outperforms RF technology by many features such as absence of interference with nearby electronic devices and RF circuits, available infrastructure, license-free bandwidth, privacy and security [3].

Moreover, other all-optical devices like photonic crystals show a promising performance regarding integration ability and power consumptions, they tend to have a very complex system design compared to the VLC technology [4-6].

Employing ight emitting diodes (LEDs) for VLC techniques has become a worthy approach for an optical wireless communication. LEDs offer several advantages compared to conventional incandescent sources; like extended lifetime, reduced power consumption, smaller size, high-switching rate, improved robustness, and higher durability and reliability. By taking their fast switching rate as an advantage, white LEDs can be used for VLC [7,8].

VLC technology is used in several applications, such as localization, high bitrate data broadcasting inside homes and offices, electro-magnetic interference (EMI), sensitive environments like aircraft, high speed-video streaming, traffic control systems, and underwater data transmission [9-11].

*Corresponding author at: nazzazzz@gmail.com

https://doi.org/10.24425/opelre.2020.135259

Meanwhile, effectively achieving communication and lighting requirements has become a compelling research area for indoor VLC data broadcasting [8].

However, designing an efficient/reliable VLC system tends to achieve additional objectives, such as power consumption reduction, higher operating system rates, enhanced throughput, flicker-free operation, enhanced dimming control range and levels, and system complexity reduction [7].

These objectives can be accomplished by using modulation techniques specifically designed for intensity modulation/direct detection (IM/DD) - optical wireless communication (OWC) systems. Such straight forward techniques are declared as single-carrier modulation (SCM) techniques. However, some of these techniques are not suitable for meeting such goals.

SCM techniques performance decreases due to the inter symbol interference (ISI) effect, especially at high operating bitrates. Hence, different equalization techniques are introduced as a reliable method for increasing the system overall performance at high operating bitrates [12-14]. But such a process comes at the expense of greatly increasing the system complexity; hence, multi-carrier modulation (MCM) techniques such as orthogonal frequency division multiplexing (OFDM) are introduced and compared with those equalization techniques.

Dimming control for VLC systems can be achieved by utilizing pulse-width modulation (PWM), but PWM suffers from the reduction of the overall system performance. The reduced system performance of the PWM scheme can be explained by its operation which is based on varying the duty cycle of signal pulses and transmitting the controlling signal only during the “on” period.

Hence, applying dimming control to on-off keying (OOK) signal significantly increases the system complexity, because the required data rate for achieving a reliable communication link is inversely proportional to the duty cycle. Additionally, it will require a significant increase in a transmitter power [15].

In Ref. 15, Z. Wang proposed applying dimming control to a scheme combining multi level-quadrature amplitude modulation (M-QAM) and OFDM. A modification on the conventional PWM dimming scheme is proposed in Ref. 16 to achieve an excess data transmission by combining the multi pulse-position modulation (MPPM) pulses with the M-QAM OFDM signal. The transmitted excess information will lead to the reduction of the data rate required to achieve a sustainable communication link which leads to the reduction of the overall system complexity and power consumption.

Although excess data transmission helps in achieving the previously mentioned VLC objectives as a dimmable VLC system, the previously proposed systems suffer from a major problemwhich is a variation of the operation data rate required along the dimming range to achieve an acceptable BER performance. this problem will lead to the fluctuation of the illumination levels as the data rate changes in a non-practical way.

IEEE 802.15.7 standard offers three physical (PHY) classes for VLC. PHY I and PHY II support OOK and variable PPM (VPPM). PHY III utilizes numerous optical sources with different frequencies (i.e., colours), moreover, it utilizes a certain modulation format called colour shift keying (CSK).

IEEE 802.15.7 standard modulation schemes grant a tradeoff between the supported data rates and dimming ranges. For example, for dimming conditions, modulation using OOK provides a constant dimming range and variable data rate by enhancing the compensation time, while modulation using the VPPM technique provides a constant data rate and a variable dimming range by adjusting the pulse width. Meanwhile, CSK provides faster data rates at lower optical frequencies [17-21]. Finally, unique power-saving performance with acceptable dimming performance and bandwidth requirements are considered as the main characteristics of PPM [22-23].

However, to the best of our knowledge IEEE 802.15.7 modulation techniques had never been utilized in an adaptive M-QAM OFDM based VLC system. Especially, the sub carrier-pulse-position modulation (SC-LPPM) scheme that has the unique reduced power consumption performance, while maintaining efficient illumination and communication performance with an extra advantage of design simplicity [24].

Another substantial limitation for more practical evaluation is utilizing the proposed dimming control schemes for different room topologies and lighting layouts, it is noteworthy to mention that although uniform lighting topology is utilized for several applications and environments, a lack of investigation for systems using the uniform lighting topology can be noticed due to its design complexity. Hence, it can be concluded that this analysis will result in evaluating the capabilities and limitations of the proposed dimming schemes for different lighting designs and different environmental parameters.

From the author’s point of view, combining VPPM, CSK and SC-LPPM with M-QAM OFDM can provide a comprehensive look to improve such dimming scheme performance.

In this work, a proposed combination and evaluation process for the IEEE 802.15.7 standard modulation techniques and SC-LPPM scheme with M-QAM OFDM will be presented, at different lighting topologies (i.e., distinctive lighting layout and uniform lighting layout), followed by the evaluation of the proposed techniques at the worst location for the proposed room layout. Then, an optimization process for M-QAM levels will be presented to provide a real-life illumination performance for various dimming ranges while maintaining a power-saving performance. That will result in identifying the combination technique capable of achieving the optimum performance with M-QAM OFDM, and most of the VLC systems design aspects.

The presented investigation will be concluded with the evaluation of the illumination performance for the dimming range and operation system rate, then evaluating the illumination across the presented room topologies.

In the presented work, the system environment for both distinctive and uniform lighting layout, with a detailed mathematical background for dimming control in VLC, excess data transmission, and the proposed merging for IEEE 802.15.7 modulation techniques with M-QAM OFDM is presented in section 2. Meanwhile, section 3

contains a detailed discussion for the required data rates, required receiver sensitivity (Rx), required transmitter power, and illumination performance across the presented room topologies. Finally, a conclusion for the obtained results will be presented in section 4.

2. System model, design, parameters, and specifications

2.1 System environment

Two scenarios are considered for the evaluation process (distinct and uniform lighting systems), within a (5 m × 5 m × 3 m) room the Rx is assumed to be at a height of 0.85 m. For distinctive lighting topology, by taking a quadrant of the room (since the room and lighting geometry are symmetrical), the room corners are defined as (0.2 m × 0.2 m) and the location under the light source is (1.25 m × 1.25 m).

The distinct lighting system uses i identical LED lamps which are equally spaced on the ceiling of the room at a center position of (1.25, 1.25, 2.5), (1.25, 3.75, 2.5), (3.75, 1.25, 2.5), (3.75, 3.75, 2.5), each LED lamp contains 3600 (60 × 60) LED chips arranged in a square array pattern as shown in Fig. 1(a).

A triangular lighting layout is used for the uniform lighting system [25]. The triangular array consists of 500 (20 × 25) LED chips, distributed as an equilateral triangle with a side length of 0.24 m and spaced on the ceiling of the room, as indicated in Fig. 1(b).

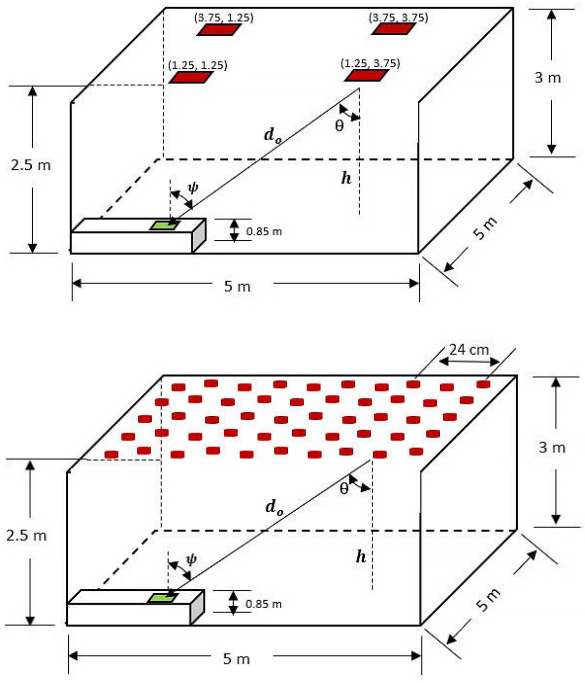

Fig. 1. Room configuration for (a) distinctive lighting layout, (b) uniform lighting layout

2.2 Dimming control in VLC system

The transmitted power irradiated by the LED source determines the optical communication channel signal strength. Hence, for a wireless optical channel, the optical power received by the photodiode can be expressed as follows [8]:

$$P_j^r = \sum_{i=1}^{I} (H(0) \cdot P_i^t), \tag{1}$$

where P_j^r is the sumation of the received optical power at workplace j from the all i^{th} sources, and $H(0)$ is the channel response which can be obtained for a LOS channel through [8]:

$$H(0) = \frac{A_{PD}\,(m+1)}{2\pi d_o^2}\, T(\theta)\, g(\theta)\, cos^m\, \theta\ cos\, \psi, \tag{2}$$

where A_{PD} is the photodiode effective area, m is the Lambert coefficient, d_o is the distance between the LED source and the Rx, θ is the angle of irradiance, and ψ is the angle of incidence, $T(\theta)$ is the optical filter gain, and $g(\theta)$ is the concentrator gain. Hence, the optical power received from a directed channel can be written as [7,8]:

$$P_j^r = \begin{cases} P_i^t \cdot \dfrac{A_{PD}\,(m+1)}{2\pi d_o^2}\, T(\theta)\, g(\theta)\, cos^m\, \theta\, cos\, \psi\,, & \theta \le FOV \\ 0, \qquad \theta > FOV, \end{cases} \tag{3}$$

where FOV is the field of view.

At the receiver end, the DC component of the signal detected by the photodetector is filtered out and by assuming a Gaussian noise, the SNR of the output electrical signal is given by [16]:

$$SNR = \frac{\overline{f(t)^2}\left(R_r P_j^r M_{index}\right)^2}{\sigma^2}, \tag{4}$$

where R_r is the responsivity of the PD, σ^2 is the noise variance, M_{index} is the modulation index, $f(t)$ is the normalized signal, and $\overline{f(t)^2}$ is its average power. Under the assumption that the noise variance consists of shot and thermal noise added together [26]:

$$\sigma^2 = \sigma_{shot}^2 + \sigma_{thermal}^2 \tag{5}$$

$$\sigma_{shot}^2 = 2q\left[R\left[P_j^r\left(1 + \left(M_{index}\overline{f(t)}\right)^2\right)\right] + I_{bg} I_2\right] B \tag{6}$$

$$\sigma_{thermal}^2 = 8\pi k T_k \eta A_{PD} B^2 \left(\frac{I_2}{G} + \frac{2\pi\Gamma\eta A_{PD} B I_3}{g_m}\right), \tag{7}$$

where $\left[P_j^r\left(1 + \left(M_{index}\overline{f(t)}\right)^2\right)\right]$ is the total received power, R is the transmitted symbol rate, q is the electron charge, T_k represents the absolute temperature, k is the Boltzmann constant, I_{bg} is the background current, I_2 and I_3 constants represents the noise bandwidth factor, B is the equivalent noise bandwidth, η is the fixed capacitance, Γ is the field-effect transistor channel noise factor, G is the open loop voltage gain, and g_m is the field-effect transconductance.

As previously discussed in section 1, in a PWM dimming scheme, the control signal is transmitted only during the 'on' period. Hence, for the OOK signal, the symbol rate required to achieve a reliable communication link is inversely proportional to the duty cycle (D_c), which can be presented as [15,16]:

$$R_{req.} = \frac{R_o}{D_c}, \qquad 0 < D_c \leq 1, \tag{8}$$

where R_o is the initial data rate and $R_{req.}$ is the symbol rate required after applying the dimming scheme. From Eq. (8), it can be indicated that the data rate required to sustain a reliable communication link will increase up to 10 times the original system data rate as the duty cycle decreases to 0.1 (i.e., 10%).

Adaptive M-QAM OFDM method was introduced to solve such problem by adjusting the number of points in each signal constellation (M), making sure that the number of transmitted bits is constant, and the required data rate. is not larger than the original symbol rate. Hence:

$$R_{req.} = \frac{M_o R_o}{M_1 D_c}, \qquad 0 < D_c \leq 1, \tag{9}$$

where M_0 is the initial number of points in each signal constellation and M_1 is the adaptive number of points in each signal constellation.

BER of the M-QAM modulation scheme depends on M, total received power, and noise variance as a function of the symbol rate; hence, it can be presented as [15]:

$$BER \leq 0.2\, exp\left[\frac{-1.5\,\overline{f(t)^2}\left(R_r P_j^r M_{index}\right)^2}{(M-1)\,\sigma^2(P_j^r)}\right]. \tag{10}$$

Forward error correction codes (FEC) like Reed-Solomon code are usually implemented in VLC systems, hence, a BER of 10^{-3} or less (i.e., preferably less than 10^{-3}) is usually required to achieve a reliable communication link. Therefore, the receiver sensitivity P_{sen}^r required to achieve the targeted BER ($BER|_{req.}$) can be presented as:

$$P_{sen}^r = \frac{1}{R_r\, M_{index}} \sqrt{\frac{ln\left(\frac{BER|_{req.}}{0.2}\right)(1-M)\,\sigma^2(P_{sen}^r)}{1.5\,\overline{f(t)^2}}}. \tag{11}$$

By observing Eqs. (4) – (6) and (10), it can be found that by reducing the duty cycle (i.e., dimming control), will increase the required symbol rate R which leads to increase in the noise variance; resulting in pushing up the receiver sensitivity requirement and transmitter power requirements. Hence, one can safely assume that increasing the duty cycle or reducing the data rate will ensure a constant data transmission. The required LED lamp power $P_{req.}^t$ can be obtained from Eq. (10) as follows:

$$P_{req.}^t = \frac{1}{R_r\, H(0)\, M_{index}} \sqrt{\frac{\ln\left(\frac{BER|_{req.}}{0.2}\right)(1-M)\,\sigma^2(P_j^r)}{1.5\,\overline{f(t)^2}}}. \tag{12}$$

2.3 Combining VPPM, CSK and SC- LPPM with M-QAM OFDM

Dimming control results in an increase in the symbol rate required to achieve a certain BER performance needed to sustain a reliable communication link. Hence, an excess data transmission technique was introduced in Ref. 16 using MPPM with M-QAM OFDM, the excess data transmission leads to the reduction of the increased symbol rate. Hence, it leads to the enhancement of the required receiver sensitivity.

The excess data rate contributed by VPPM [27], CSK [20], MPPM [16], and SC-LPPM [28] can be described as:

$$R_{VPPM} = \begin{cases} b\, d_1 & , \quad 0 < d_1 < 0.5 \\ b\,(1 - d_1) & , \quad 0.5 \leq d_1 < 1 \end{cases} \tag{13}$$

$$R_{CSK} = b\, log_2(L_{CSK}) \tag{14}$$

$$R_{MPPM} = \frac{log_2(C_w^p)}{T_{PWM}} \tag{15}$$

$$R_{SC-LPPM} = \frac{\log_2(L_{SC-LPPM})}{L_{SC-LPPM} \cdot T_{PWM}}. \tag{16}$$

Where b is the optical clock rate, d_1 is the duration of VPPM (i.e., the ratio between the average power and the peak power of the signal), T_{PWM} is the period of the original PWM signal, L_{CSK} represents the number of points on the CSK constellation, C_w^p is the number of patterns in each MPPM symbol, n is the total number of slots of an MPPM symbol, p is the number of pulses in each MPPM symbol, and $L_{SC-LPPM}$ is the number of time slots of the SC-LPPM symbol interval.

The proposed dimming scheme is shown in Fig. 2. First, the bipolar data stream is mapped through PWM, VPPM, CSK, MPPM, or SC-LPPM blocks, then the signal is modulated through the M-QAM OFDM block (i.e., DC-Biased optical (DCO-) or asymmetrically clipped optical (ACO-) OFDM. The optical signal is transmitted through the AWGN channel by the LED source. After the optical signal is received by the PD, a reverse process is performed to demodulate the signal resulting in decomposing it into two main components: The M-QAM OFDM signal and the dimming scheme (i.e., PWM, VPPM, CSK, MPPM, or SC-LPPM) signal followed by the signal recovery.

The output signal (i.e., current) driving the LED source $s(t)$ can be defined as the ordinary product of the OFDM signal $x(t)$ and the dimming scheme signal $y(t)$, hence, it can be written as [29]:

$$s(t) = x(t) \cdot y(t). \tag{17}$$

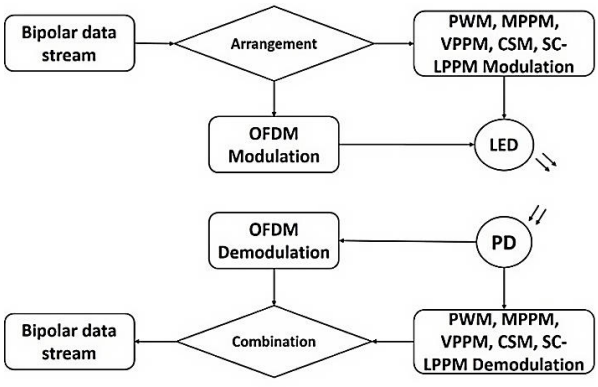

Fig. 2. Block diagram for conventional and proposed dimming schemes utilizing M-QAM OFDM

The OFDM signal $x(t)$ is composed of N subcarriers and can be represented as:

$$x(t) = Real(\sum_{c=0}^{N-1} s_c\, e^{-j2\pi f_c t}), \quad (18)$$

where f_c is the frequency of each subcarrier and s_c is the M-QAM signal modulated on the carrier frequency f_c. A generalization of the $y(t)$ spectrum for all presented schemes can be presented as [29]:

$$Y(f) = \frac{1}{T}\int_0^T y(t)e^{-j2\pi f_c t}\, dt. \quad (19)$$

Due to the LED limitations, it is safe to assume that a high-frequency component of the signal carrying the OFDM signal will be suppressed, resulting in the distortion of the signal $Y(f)$. Hence, by using pre-distortion techniques, the effect of inter-carrier interference (ICI) and $Y(f)$ distortion can be eliminated. Moreover, orthogonality and guard intervals of the OFDM signal between the transmitted subcarriers eliminate the multipath effect.

However, the length of the OFDM symbol should be properly designed. As the increase in the length of the OFDM symbol will result in a delay of the signal processing, it will reduce the overall system speed. While decreasing the OFDM symbol length could result in degrading the transmission efficiency due to the reduction of the guard interval.

2.4 System specifications

Considering the room data mentioned in section 2.1, extra LED parameters are listed in Table 1 to ensure reliable lighting and communication performance.

According to the IEEE 802.15.7 standard for VLC systems, each PHY modulation scheme has a different optical clock rate [19,20], these optical clock rates are presented in Table 2.

3. Performance exploration, evaluation and discussion

3.1 Introduction

By taking the room data, topology and LED parameters presented in section 2.1 and section 2.4 into consideration, symbol rate performance, receiver sensitivity, and required Tx power can be considered as a key parameter required to design a dimmable VLC system that can maintain a reliable communication link. An investigation and evaluation of the combination process between MQAM-OFDM with PWM, MPPM, VPPM, CSK, and SC-LPPM schemes will be carried for different dimming ranges in section 3.2. Followed by a comparison between the combination process of different modulation techniques with M-QAM OFDM are presented in the previous literature and the proposed merging process presented in this work.

In section 3.4, an illumination performance study will be carried for the usable range of operating system rates, followed by an investigation of the overall illumination performance for the entire room at different lighting topologies. This investigation is critical to determine the proposed system performance across the entire room.

It is noteworthy to mention that this work is based on the mathematical model presented in section 2, meanwhile the previous literature investigated the performance of other types for modulation and dimming schemes practically. In these studies, the authors concluded that the practical system performance shows a fair agreement with the theoretical analysis [30-32].

Table 1
Lighting systems configuration, noise parameters, LED, and photodiode characteristics.

Category	Parameters	Value	
		Distinctive lighting layout	**Uniform lighting layout**
Lighting configuration			
	Number of LEDs	3600	500
	LED distribution	60 × 60	20 × 25
	LED spacing	0.09 m	0.24 m
	Center position	(1.25, 1.25), (1.25, 3.75), (3.75, 1.25), (3.75, 3.75)	(2.5, 2.5)
Noise parameters			
	Background current (I_{bg})	5100 μA	
	Noise bandwidth factor (I_2)	0.562	
	Field-effect transistor (FET)	30 mS	
	FET channel noise factor (Γ)	1.5	
	Fixed capacitance (η)	112 pF/cm^2	
	Open-loop voltage gain (G)	10	
	I_3	0.0868	
Source			
	LED transmitted power	20 mW	
	Semi-angle half power ($\theta_{1/2}$)	60°	
	Center luminous intensity	0.73 cd	
	Power spectrum density	10^{-21}	
Receiver			
	Physical area (A_{PD})	1 cm^2	
	Field of view (FOV)	170°	
	Responsivity (R)	1 A/W	
	Filter gain (T_s)	1	
	Concentrator gain (g)	1	
	Elevation	90°	

Table 2
IEEE 802.15.7 PHY operation modes.

PHY layer	Modulation scheme	Optical clock rate
PHY I	VPPM	400 kHz
PHY II	VPPM	3.75 MHz
		7.5 MHz
	4-CSK	12 MHz
	8-CSK	
PHY III	4-CSK	
	8-CSK	24 MHz
	16-CSK	

3.2 *Performance evaluation for the proposed dimming schemes using M-QAM OFDM*

The BER required to maintain a reliable communication link is set to 10^{-3}, and the original transmission data rate is set to 50 Mb/s [15]. To guarantee a flicker-free performance, the frequency of PWM is set to 200 kHz, while at the receiver a blue light filter can be used to extend the modulation bandwidth to 20 MHz [33].

As mentioned in section 2.2, decreasing the duty cycle will increase the required symbol rate to sustain a reliable communication link. Hence, the required data rate at 10% dimming will be equal to 500 Mb/s which results in a more complex circuit design. Therefore, an adaptive M-QAM technique; where, M is adjusted for the minimum LED power is introduced in Refs. 15 and 16 leading to the optimization of the required data rate, the variable M is given in Table 3.

Table 3
Adaptive M-QAM levels (M) [15,16].

Duty cycle	0.2	0.3	0.4	0.5	0.6	0.7	0.8	0.9	1
M-QAM	1024	128	32	16	16	8	8	8	4

The required symbol rate for the schemes combining (PWM, MPPM, VPPM, CSK, and SC-LPPM) signal with M-QAM OFDM is presented in Fig. 3. From Fig. 3 it can be indicated that the required M-QAM symbol rate according to the values of M presented in Table 3 is maintained between 50 Msymbol/s and 28 Msymbol/s.

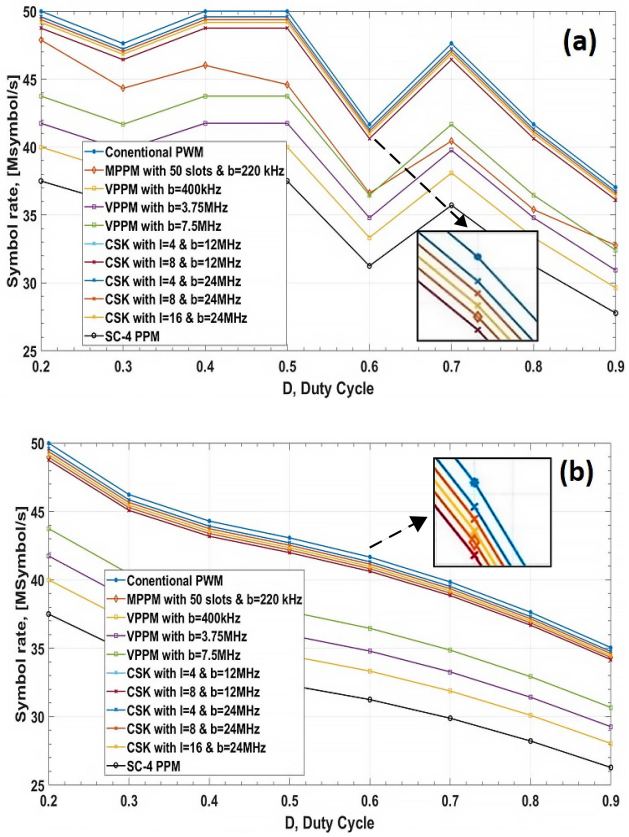

Fig. 3. Required symbol rate for a reliable transmission for (a) conventional adaptive M-QAM levels, (b) proposed adaptive M-QAM levels.

Figure 3(a) shows that the required symbol rate overall performance is enhanced by increasing the duty cycle. For a specific duty cycle, it is shown that PWM shows the lowest performance regarding the symbol rate requirement. MPPM shows a moderate performance when compared to CSK and VPPM, while the optimum performance of 37.5 Msybmol/s at $D = 0.2$ and 28 Msymbol/s at $D = 0.9$ are achieved by the SC-LPPM scheme.

However, it is noticed that the symbol rate dynamically changes along with the dimming range, this change will result in an undesirable fluctuation in the illumination levels within a given room. Hence, in Table 4 we introduced new values for M which will guarantee a continuous change in the required symbol rate, resulting in a continuous illumination performance from the lighting source.

Table 4
Introduced adaptive M-QAM levels (M).

Duty cycle	0.2	0.3	0.4	0.5	0.6	0.7	0.8	0.9	1
M-QAM	1024	128	64	32	16	8	8	8	4

Figure 3(b) shows the required symbol rate performance for the presented scheme. From Fig. 3(b), it is shown that symbol rate requirement performance changes gradually when compared to Fig. 3(a) while maintaining the same range between 50 Msymbol/s and 28 Msymbol/s. Moreover, PWM, CSK, VPPM, MPPM, and SC-LPPM shows the same performance when compared to each other. Hence, it can be predicted that the illumination will continuously change by changing the data rate as it will be discussed in the following section.

Figure 4 shows the sensitivity required for the receiver to achieve a BER performance lower than 10^{-3}. Hence, it can be indicated that increasing the duty cycle results in enhancing the sensitivity requirements which shows a fair agreement with the results extracted from Fig. 3 due to the enhancement (i.e., reduction) of the required symbol rate. It can be indicated from Fig. 4 that higher M-QAM levels will result in pushing up the receiver sensitivity requirements. Hence, for the energy optimization lower M-QAM levels should be chosen.

Figure 4(a), shows the sensitivity requirement for the distinctive lighting topology. From Fig. 4(a) it is shown that the sensitivity requirement of PWM enhances from −19.83 dBm to −31.13 dBm at $D = 0.2$ and $D = 0.9$, respectively. Moreover, it is shown that the MPPM scheme shows a better performance than CSK at $L = 4$ and $b = 12$ MHz, $b = 24$ MHz, and $L = 8$ and $b = 24$ MHz, while CSK at $L = 8$ and an optical clock rate of 12 MHz shows a slight enhancement over MPPM scheme. Another observation can be made that CSK at $L = 16$ and $b = 24$ MHz shows an identical performance to CSK at $L = 4$ and $b = 12$ MHz.

SC-4 PPM shows the optimum performance of −20.45 dBm at $D = 0.2$ and −31.76 dBm at $D = 0.9$ when compared to VPPM which shows a better sensitivity requirement performance when compared to PWM, MPPM and CSK. By observing the received power detected by the PD, it can be indicated that for a distinctive lighting system; a dimming range up to 30% can be implemented.

The same behavior can be indicated for the uniform lighting topology from Fig. 4(b). The overall system sensitivity requirement shows a lower performance when compared to the overall performance of distinctive lighting topology. The sensitivity requirement of PWM increases from −35.4 dBm at $D = 0.9$ to −24.1 dBm at $D = 0.2$.

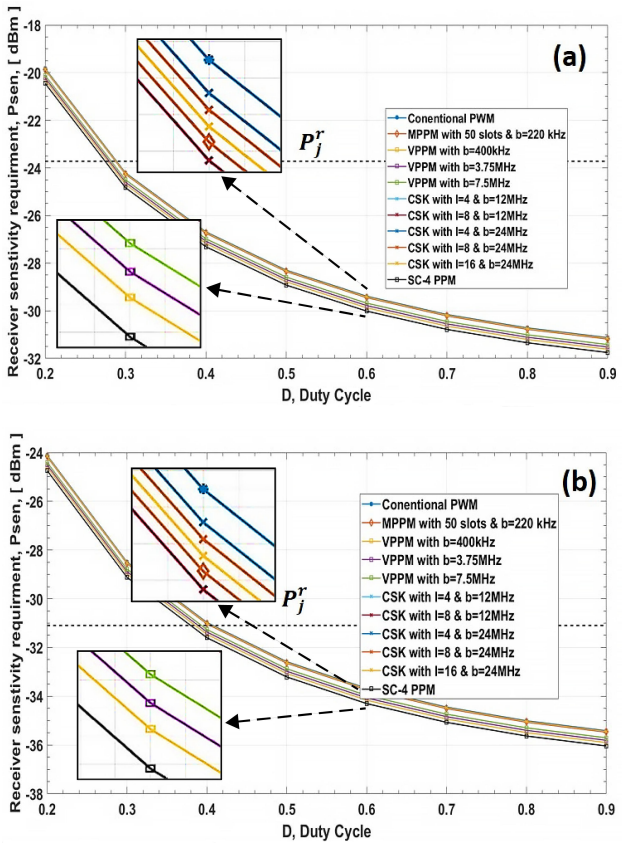

Fig. 4. Receiver sensitivity requirements for (a) distinctive lighting layout, (b) uniform lighting layout

Once again, SC-4PPM shows an optimum performance regarding the *Rx* sensitivity requirements, as the receiver sensitivity performance of −24.74 dBm and −36 dBm at $D = 0.2$, and $D = 0.9$, respectively is achieved, with an enhancement of 0.63 dBm compared to PWM. Also, it is observed that all presented modulation scheme shows the same behavior when compared to PWM as in Fig. 4(a). Meanwhile, Figure 4(b) shows that a dimming range of up to 40% can be implemented for the uniform lighting topology.

The required LED power to maintain a BER of 10^{-3} [15,16] (i.e., reliable communication link) is shown in Fig. 5. From Fig. 5(a), it is observed that the required LED power increases as the duty cycle decreases for all of the proposed combination schemes. The required LED power for PWM increases from 0.317 W to 4.288 W, as the duty cycle decreases from 0.9 to 0.2, respectively. While for the MPPM scheme the required LED power enhances by a small margin of 0.045 W at a duty cycle of 0.2. CSK scheme shows almost identical performance as the MPPM scheme. While VPPM scheme shows an overall enhancement when compared to PWM, MPPM and CSK, moreover it is shown that the performance of VPPM enhances as the optical clock rate decreases but with a small margin, VPPM with $b = 400$ kHz required

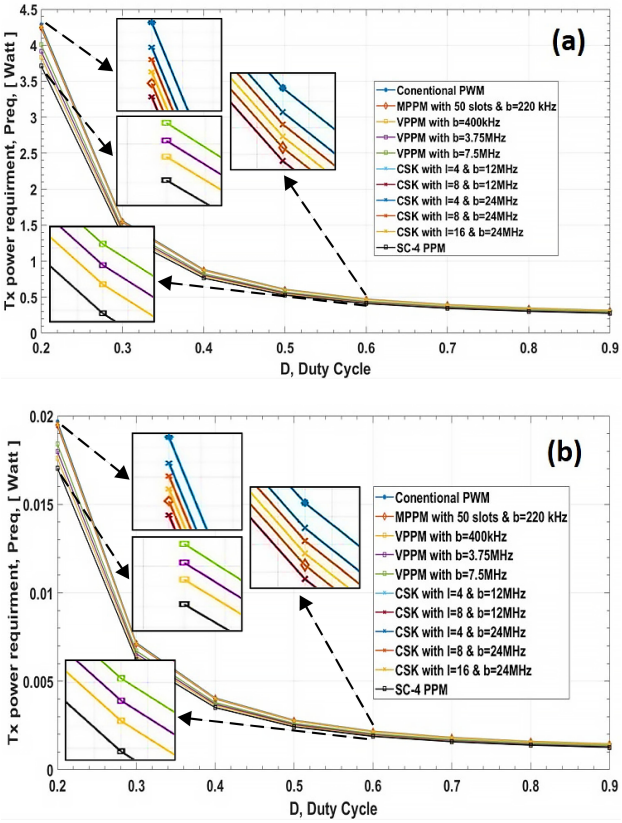

Fig. 5. Transmitter power requirement for (a) distinctive lighting layout, (b) uniform lighting layout.

LED power decreases from 4.011 W at $D = 0.2$ to 0.297 W at $D = 0.9$. Finally, SC-4 PPM shows an optimum performance regarding the required LED power of 3.713 W at a duty cycle of 0.2 and 0.2749 at a duty cycle of 0.9.

For the uniform lighting topology and from Fig. 5(b), it is shown that the overall behavior is almost identical to the distinctive lighting layout. From Fig. 5(b) it can be indicated that the required LED power for PWM enhances from 0.0196 W to 0.00145 W when the duty cycle increases from 0.2 to 0.9, respectively. MPPM and CSK show almost the same performance as in Fig. 5(a) as the required LED power increases from 0.00142 W at $D = 0.9$ to 0.0194 W at $D = 0.2$, also it is shown that the performance enhancement is not by far when compared to PWM. VPPM at $b = 400$ kHz shown a small enhancement as the required LED power decreases from 0.0176 W to 0.0013 W at $D = 0.2$ and $D = 0.9$, respectively. Once again SC-4 PPM shows an optimum power-saving performance as the required LED power enhances from 0.017 W at $D = 0.2$ and 0.0012 at $D = 0.9$.

It is noteworthy to mention that for the uniform lighting system the required LED power that is shown in Fig. 5(b) is calculated for a single LED. Hence, for the presented room layout which contains 500 LED sources the total required power for SC-4 PPM will be equal to 8.5 W.

Another observation can be made from Fig. 5 that the required LED power for all the proposed schemes shows almost the same performance at a large duty cycle (i.e., $D = 0.9$) and the more performance improvement can be observed at a smaller duty cycle (i.e., $D = 0.2$). Moreover, for the dimming control to achieve a BER of 10^{-3} the

required LED power should be larger than 4.288 W and 8.5 W for distinctive and uniform lighting topologies, respectively.

3.3 *Comparison between merging techniques presented in the previous literature and the proposed combination with M-QAM OFDM*

As mentioned before, the previous literature investigated the performance of merging M-QAM OFDM with different modulation techniques. Hence, in this section, Table 5 presents a comparison between the previously investigated combination process and the proposed combination process between the PWM, MPPM, VPPM, CSK, and SC-LPPM regarding the required symbol rate, required receiver sensitivity, and the required transmitter power will be carried for the adaptive M-QAM levels presented in Table 4.

It is shown in Table 5, regarding the distinctive lighting topology the M-QAM levels resulted in the overall enhancement of the required symbol rate, receiver sensitivity and transmitter power for PWM, as well as MPPM. While the proposed combination between VPPM, CSK and SC-LPPM with M-QAM OFDM shows a further improvement for the same parameters, especially SC-LPPM shows the optimum performance for both distinctive and uniform lighting topologies.

3.4 *Investigating the illumination performance of SC-LPPM*

From section 3.2 and section 3.3, it can be indicated that SC-LPPM shows the optimum performance regarding the required data rate, required receiver sensitivity and required transmitter power. Hence, to adequately investigate the performance of a dimming scheme, the illumination performance over the operating bitrate should be investigated. Moreover, the illumination distribution across the proposed room topologies is evaluated to investigate the illumination levels at the room corners and under the lighting sources. This study gives a real-life presentation to the illumination performance of the SC-LPPM scheme.

For SC-LPPM, when the input waveform has a DC component with a maximum amplitude; the output luminous flux generated by a LED lamp can be presented as [28,34]:

$$\varphi_i = N_{i/T} \cdot \varphi_{max}, \tag{20}$$

where i is the lamp index, $N_{i/T}$ is the brightness factor per symbol duration and φ_{max} is the maximum luminous flux generated by each LED.

Hence, the brightness factor can be described as [28,34]:

$$N_{i/T} = (\tau_a (a_i + c_i) + \tau_b b), \tag{21}$$

where τ_a and τ_b are $T_{Slot/2}$ and $3T_{Slot}$, respectively and T_{Slot} is the time slot duration.

Hence, the output luminous flux generated by a LED lamp can be described as:

$$\varphi_i = (\tau_1(a_i + c_i) + \tau_2 b)\, \varphi_{\max}, \tag{22}$$

where $(c - a)$ is the optical signal amplitude, and b is the amplitude of the direct current component. Since illuminance is the brightness level of the illuminated surface and by adding all of the LED lamps generated illuminance, the illuminance level at the workplace j can be obtained. Hence, the total illuminance level can be presented as [28,34]:

$$E_j = \sum_{i=1}^{I} e_{ij}, \tag{23}$$

where e_{ij} is the illuminance received at the workplace j from the LED lamp i.

Table 5
Comparison of modulation techniques merged with M-QAM OFDM.

Ref.	Evaluated techniques	Room topology								
			Distinctive				Uniform			
		No. of LED lamps	$R_{req.}$ [Msymbol/s]		P^r_{sen} [dBm]	$P^t_{req.}$ [Watt]	$R_{req.}$ [Msymbol/s]		P^r_{sen} [dBm]	$P^t_{req.}$ [mw/ LED]
			Min.	Max.	D = 0.2	D = 0.2	Min.	Max.	D = 0.2	D = 0.2
15	PWM	1	26.5	50	NA	4.1	NA	NA	NA	NA
16	PWM	1	42	50	−11.6	16.9	NA	NA	NA	NA
	MPPM	1	37	49	−13.23	11.7	NA	NA	NA	NA
In this work	PWM	4	35	50	−19.83	4.28	35	50	−24.10	19.68
	MPPM	4	34.3	49	−19.87	4.24	34.3	49	−24.16	19.48
	VPPM	4	28	40	−20.31	3.83	28	40	−24.6	17.61
	CSK	4	34.5	49.17	−19.88	4.23	34.5	49.17	−24.17	19.44
	SC-LPPM	4	26.3	37.5	−20.45	3.71	26.3	37.5	−24.74	17.05

Assuming that the source has a Lambert radiation characteristic, e_{ij} can be expressed as:

$$e_{ij} = \frac{(m+1)\varphi_i}{2\pi d_o^2} \cos^m \theta \ \cos \psi. \quad (24)$$

By using the proposed M-QAM levels presented in Table 4, Eqs. (22) – (24), Figure 6 shows the received illumination at the *Rx* location presented in section 2.1, it can be observed that the illumination performance smoothly enhances as the operating bit rate decreases. As previously discussed in Fig. 3(b), the required symbol rate enhances (i.e., decreases) from 37.5 Msymbol/s to 26.3 Msymbol/s as the duty cycle increases from 0.2 to 0.9, respectively; hence, the total received illumination will enhance as the required operation symbol rate decreases.

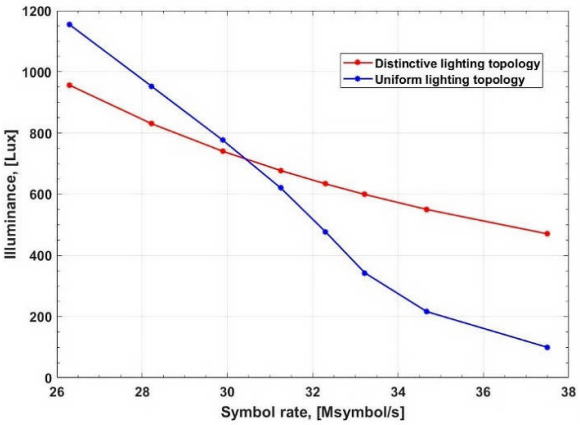

Fig. 6. Illumination performance under the operating symbol rates for distinctive and uniform lighting topologies.

Figure 6 shows the illumination performance for SC-LPPM of the proposed distinctive lighting and uniform lighting topologies. For the distinctive lighting topology, the illumination smoothly decreases from 957 lux to 470 lux as the required operation symbol rate increases from 37.5 Msymbol/s to 26.3 Msymbol/s.

Meanwhile, uniform lighting layout shows a better performance of 1155 lux compared to the distinctive lighting layout at the lower operating symbol rates. However, as the symbol rate increases the illumination performance of the uniform lighting layout achieves an illumination level of 100 lux at a symbol rate of 37.5 Msymbol/s which is lower than the distinctive lighting layout.

Hence, it can be concluded from Fig. 6 that the illumination performance of the uniform lighting layout cannot achieve the required illumination standard of 400 lux required for a typical room [8], at higher operating symbol rates.

From Fig. 6, the uniform lighting topology achieves an illumination performance of 477 lux at a symbol rate of 32.3 Msymbol/s which corresponds to a duty cycle of 0.5 (i.e., 50% dimming). Such observation represents the limitations of the proposed dimming scheme combined with M-QAM OFDM for the uniform lighting topology.

Figure 7 represents the illumination distribution within the proposed room topologies (i.e., distinctive and uniform lighting layout). It is noteworthy to mention that

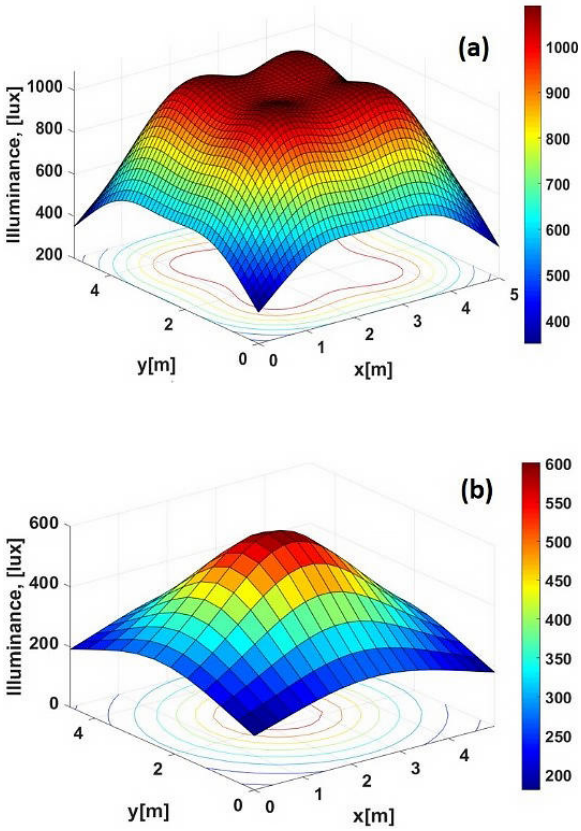

Fig. 7. Received illumination for (a) distinctive lighting layout, (b) uniform lighting layout.

the receiving surface is divided into 20 × 20 segments to form a grid that helps in the calculation of the illumination within the proposed room topologies. Moreover, to adequately investigate the lighting performance of the proposed dimming scheme; the investigation is done at the highest required operating symbol rate.

It can be indicated from Fig. 7(a) that the illumination performance for the distinctive lighting topology decreases from 1090 lux under the light sources to 394 lux as the Rx moves towards the room corners. Hence, it is safe to assume that locating the receiver between 1 m × 1 m will meet the targeted illumination standard of 400 lux [8].

Figure 7(b) shows the illumination performance of the uniform lighting topology, it can be indicated that the illumination decreases from 600 lux at the receiver location to 180 lux at the farthest point of the room. Moreover, it can be indicated that the Rx will receive the illumination largest component from the LED sources placed on top of it, while the received illumination levels decrease as the LED sources get farther away from the Rx, hence it can be concluded that a constant illumination level will be received along with the room if the Rx is reallocated.

4. Conclusions

The presented work investigates VLC dimming schemes based on merging VPPM, CSK and SC-LPPM with M-QAM OFDM, then compared with conventional schemes combining PWM and MPPM with M-QAM OFDM. The investigation process is performed for

different lighting layouts. SC-4 PPM achieves an optimum performance for the symbol rate requirement of 37.5 Msymbol/s at $D = 0.2$ and 28 Msymbol/s at $D = 0.9$. Also, it shows an optimum performance for the required Rx sensitivity of −2.45 dBm, −36dBm at $D = 0.2$ and −31.76 dBm, −24.74 dBm at $D = 0.9$ for a distinctive and uniform lighting layout, respectively; while the required transmitter power decreases from 3.713 W at $D = 0.2$ to 0.2749 W at $D = 0.9$ for a distinctive lighting layout, and from 0.017 W at $D = 0.2$ to 0.0012 W at $D = 0.9$ for the uniform lighting layout.

An illumination study is performed to determine the capabilities and limitations of SC-4 PPM with the M-QAM OFDM scheme along with the operation range of a symbol rate. For distinctive lighting layout, although the proposed merging scheme showed a minimum illumination of 470 lux at the maximum operating symbol rate, the dimming capability of the scheme is up to 30% can be implemented due to the sensitivity requirements, while the generated illumination for the uniform lighting layout scheme showed a decrease in performance which allows a dimming range up to 50%.

Finally, investigating the illumination performance across the proposed room shows that the distinctive lighting layout can provide an illumination up to 1090 lux under the light sources and 394 lux at the room corners but with the cost of an increased number of LEDs. Meanwhile the uniform lighting layout shows lower performance for the achieved illumination of 600 lux across the room.

References

[1] Jovicic, A., Li, J. & Richardson, T. Visible light communication: opportunities, challenges and the path to market. *IEEE Commun. Mag.* **51** (12), 26–32 (2013).

[2] O'Brien, D. & Katz, M. Optical wireless communications within fourth-generation wireless systems. *J. Opt. Netw.* **4** (6), 312–322 (2005).

[3] Grobe, L. *et al*. High-speed visible light communication systems. *IEEE Commun. Mag.* **51** (12), 60–66 (2013).

[4] Mostafa, T. S., Mohammed, N. A. & El-Rabaie, E. S. M. Ultracompact ultrafast-switching-speed all-optical 4×2 encoder based on photonic crystal. *J. Comput. Electron.* **18**, 279–292 (2019). https://doi.org/10.1007/s10825-018-1278-6

[5] Mostafa, T. S., Mohammed, N. A. & El-Rabaie, E. S. M. Ultra-high bit rate all-optical AND/OR logic gates based on photonic crystal with multi-wavelength simultaneous operation. *J. Mod. Opt.* **66**, 1005–1016 (2019). https://doi.org/10.1080/09500340.2019.1598587

[6] Mohammed, N. A., Hamed, M. M., Khalaf, A. A., Alsayyari, A. & EL-Rabaie, S. High-sensitivity ultra-quality factor and remarkable compact blood components biomedical sensor based on nanocavity coupled photonic crystal. *Results Phys.* **14**, 102478 (2019). https://doi.org/10.1016/j.rinp.2019.102478

[7] Mohammed, N. A. & Elkarim, M. A. Exploring the effect of diffuse reflection on indoor localization systems based on RSSI-VLC. *Opt. Express.* **23** (16), 20297–20313 (2015).

[8] Din, I. & Kim, H. Energy-efficient brightness control and data transmission for visible light communication. *IEEE Photon. Technol. Lett.* **26** (8), 781–784 (2014).

[9] Quintana, C., Guerra, V., Rufo, J., Rabadan, J. & Perez-Jimenez, R. Reading lamp-based visible light communication system for in-flight entertainment. *IEEE Trans. Consum. Electron.* **59** (1), 31–37 (2013).

[10] Yamazato, T. *et al*. Image-sensor-based visible light communication for automotive applications. *IEEE Commun. Mag.* **52** (7), 88–97 (2014).

[11] Rust, I. C. & Asada, H. H. A dual-use visible light approach to integrated communication and localization of underwater robots with application to non-destructive nuclear reactor inspection. in *IEEE International Conference on Robotics and Automation (ICRA 2012)*, 2445–2450 (2012).

[12] Kahn, J. M. & Barry, J. R. Wireless infrared communications. *Proc. IEEE Inst. Electr. Electron Eng.* **85** (2), 265–298 (1997).

[13] Carruther, J. B. & Kahn, J. M. Angle diversity for nondirected wireless infrared communication. *IEEE Trans. Commun.* **48** (6), 960–969 (2000).

[14] Proakis, J. G. *Digital Communications*. 4th ed. New York, USA: McGraw Hill (2000).

[15] Wang, Z. *et al*. Performance of dimming control scheme in visible light communication system. *Opt. Express*. **20** (17), 18861–18868 (2012).

[16] You, X., Chen, J., Zheng, H. & Yu, C. Efficient data transmission using MPPM dimming control in indoor visible light communication. *IEEE Photonics J*. **7** (4), 1–12 (2015).

[17] Zafar, F., Karunatilaka, D. & Parthiban, R. Dimming schemes for visible light communication: the state of research. *IEEE Wirel. Commun.* **22** (2), 29–35 (2015).

[18] Wang, M. *et al*. Efficient coding modulation and seamless rate adaptation for visible light communications. *IEEE Wirel. Commun.* **22** (2), 86–93 (2015).

[19] Roberts, R. D. IEEE 802.15.7 visible light communication: modulation schemes and dimming support. *IEEE Commun. Mag.* **50** (3), 72–82 (2012).

[20] Bai, B., He, Q., Xu, Z. & Fan., Y. The color shift key modulation with non-uniform signaling visible light communication. in *IEEE International Conference on Communications in China Workshops (ICCC 2012)*, 37–42 (2012).

[21] Pergoloni, S. *et.al*. Merging color shift keying and complementary pulse position modulation for visible light illumination and communication. *J. Light. Technol.* **33** (1), 192–200 (2015).

[22] Knutson, C. D. & Brown, J. M. *IrDA Principles and Protocols.* (MCL Press, 2004).

[23] Watson, M. *Foreword. In IrDA Principles and Protocols.* 1: vii–viii (MCL Press, 2004).

[24] Sugiyama, H., Haruyama, S. & Nakagawa, M. Brightness Control Methods for Illumination and Visible-Light Communication Systems. in *2007 Third International Conference on Wireless and Mobile Communications (ICWMC'07)* 78 (2007). https://doi.org/10.1109/ICWMC.2007.26

[25] Elkarim, M. A, Mohammed, N. A. & Aly, M. H. Exploring the performance of indoor localization systems based on VLC-RSSI, including the effect of NLOS components using two light-emitting diode lighting systems. *Opt. Eng.* **54** (10), 105110 (2015).

[26] Komine, T. & Nakagawa, M. Fundamental analysis for visible-light communication system using LED lights. *IEEE Trans. Consum. Electron.* **50** (1), 100–107 (2004).

[27] Gancarz, J. E., Elgala, H. & Little, T. D. C. Overlapping PPM for band-limited visible light communication and dimming. *J. Solid State Light*. **2** (1), 3 (2015).

[28] Mohammed, N. A. & Badawi, K. A. Design and performance evaluation for a non-line of sight VLC dimmable system based on SC-LPPM. *IEEE Access.* **6** (1), 52393–52405 (2018).

[29] Chen, J., You, X., Zheng, H. & Yu, C. Excess signal transmission with dimming control pattern in indoor visible light communication systems. in *Proc.SPIE* vol. 9270 (2014).

[30] Mao, L. *et al*. A mixed-interval multi-pulse position modulation scheme for real-time visible light communication system. *Opt. Commun.* **402**, 330–335 (2017).

[31] Kumar, N. Visible light communication system for road safety applications. Ph.D. dissertation, Dept. Elect. Eng., Aveiro Univ., Porto, Portugal (2011).

[32] Bui, T., Singh, R., O'Farrell, T. & Biagi, M. Energy-constrained slot-amplitude modulation with dimming support. *IEEE Photon. Technol. Lett.* **30** (14), 1301–1304 (2018). https://doi.org/10.1109/LPT.2018.2845670

[33] Le-Minh H. *et al*. 100-Mb/s NRZ visible light communications using a post-equalized white LED. *IEEE Photon. Technol. Lett.* **21** (15), 1063–1065 (2009).

[34] Badawi, K. A., Mohammed, N. A. & Aly, M. H. Exploring BER performance of a SC-LPPM based LOS-VLC system with distinctive lighting. *J. Optoelectron. Adv. Mater.* **20** (5-6), 290–301 (2018).